E-ISSN 2581 – 7957
P-ISSN 2277 – 3916
CVR Journal of Science and Technology, Volume 24, June 2023
DOI: 10.32377/cvrjst2418

A Numerical Study of the Effect of Viscous Dissipation on the Heat and Mass Transfer of a Rotatory Nano Fluid

Alfunsa Prathiba[1] and P. Johnson Babu[2]
[1]Sr. Asst. Professor, CVR College of Engineering/H&S(Mathematics)Department, Hyderabad, India
Email id: alphonsaperli@gmail.com
[2]Asst. Professor, St Joseph's Degree and P.G College/ Department of Physics and Electronics, Hyderabad, India
Email id: johnson.life@gmail.com

Abstract: **Viscosity dissipation is the non-reversible conversion of mechanical energy into thermal energy that occurs when a fluid performs work on neighbouring layers as a result of the impact of shear forces. Thus, the purpose of this research is to address the viscous dissipation effect on boundary layer flow of rotating incompressible Cu-Water nanofluid over an elongating surface. The model equations are transformed into a set of nonlinear ordinary differential (ODE) equations using a similarity transformation prior to getting computationally analysed using the Lobatto III A method using MATLAB. The influence of various parameters such as Eckert number, rotation porosity parameter etc on the flow properties has been analysed. The analysis discloses that with the amplification of the rotation parameter, Eckert number, nanoparticle volume fraction, and the porosity the temperature of the fluid experiences an improvement. Moreover, the velocity in the secondary direction decreases with an increase in the rotation parameter.**

Keywords: **Boundary layer, rotatory flow, viscous dissipation, porous medium, Lobatto III A method.**

I. INTRODUCTION

Viscous dissipation refers to the irreversible conversion of mechanical energy into kinetic energy that occurs as a result of fluid particle interactions. It is of importance in numerous applications such as the substantial temperature increase is found in high-velocity polymer manufacturing flows including as extrusion or injection moulding. The thin boundary layer surrounding fast aircraft experiences aerodynamic heating, which boosts skin temperature [1]. Viscosity dissipation and spontaneous convection flow were initially studied by Gebhart [2]. He found that in natural convection flows with significant gravitational effects or a liquid with a large Prandtl number, internal produced energy cannot be ignored. Hussanan et al [3] defined viscous dissipation as "the work done by a fluid on neighbouring layers due to the impact of shear forces". Nur Syamila Yusof et al.,[4] studied "the steady-state flow of a non-Newtonian fluid (Casson fluid) across an exponentially porous, slippery Riga plate with thermal radiation and magnetic field effects". They discovered that increasing the thermal and velocity slip parameters reduces the temperature. Using the Lobatto III A approach, Mohamad Shoaib et al [5] explored "heat and mass transfer in 3D radiative flow of hybrid nanofluid across a rotating disc". They discovered that temperature distribution is related to Brinkman number [5].

Heat transfer is crucial in many fields including biomedical, material science, oceanographic, nanotechnology, inorganic chemistry, and many more [6]. It is used in several technical advancements such as liquid distillation, heat exchange, and atomic controller refrigeration. In fluid mechanics, viscosity causes resistance to fluid motion, converting mechanical energy into heat energy. Thus, it is termed as internal energy shift [7]. Irfan Anjum Badruddin et al used the Finite element approach to explore the influence of viscous dissipation and heat radiation on natural convection in a porous material enclosed inside a vertical annulus tube and found that the average Nusselt number rises near the cold plate owing to increasing Ec values [8].

Nanofluid (NF) is a mixture of base fluid (water, ethanol etc) and nanoparticles. It is well known that the presence of nanomaterials alters the transporting characteristics and heat transfer efficiency in NF. The heat transmission qualities of a nanofluid are based on the mass fraction and thermophysical parameters of nanoparticles as well as the base fluid. These fluids are included in applications such as, oil exploration, metal extrusion, fiberglass polymer processing, continuous casting, plastic foil elongating and geothermal energy extraction. The thermal capacity of a NF with a permeable medium may be increased. Using nanoparticles in base liquids like oil, water, and ethylene glycol is a great way to improve heat transfer rate [9]. Research conducted on heat transfer intensification via NF can be identified in the series of the work.

In multiple procedures: such as temperature distribution, geothermal, enzymatic, nuclear reactor designs and earth sciences, there is the incorporation of convective flow in view of a porous media [10]. Permeable porous space is quite strong in subterranean systems, energy accumulating units, the circulation of water in supplies, photovoltaic reception, and so on. A large number of rotational "flows near stretchable or inextensible limits" are now being studied by academics. Zaimi et al. [11] constructed self-similar solutions for rotating viscoelastic fluid flow through an impermeable stretchable surface. Bakar et al [12] analysed "forced convection stagnation-point flow in a Darcy-Forchheimer porous medium towards a shrinking sheet". Ullah et al. [13] investigated the "effect of velocity slip on MHD Casson fluid in a porous medium with nonlinear stretching". Many researchers have engaged themselves in analysing the flow properties under various conditions in the presence of porous

Received on 09-02-2023, Revised on 29-03-2023, Accepted on 11-04-2023.

medium due to its immense industrial and geophysical applications [14]–[18].
Due to its numerous useful applications in a wide range of engineering systems, boundary layer flows with internal heat generation over stretching sheets continue to be studied [1]. To best of the knowledge of the author the impact of internal energy on the rotary $Cu + H_2O$ flow in the presence of porous medium was not addressed by the researchers. Thus, the relevance of viscous dissipation to the thermal performance across a spinning sheet is underlined in this research.

II. Modelling of the Flow

Considering a steady, laminar, incompressible $Cu + water$ NF rotating flows over an expanding sheet in the presence of internal energy as shown in Figure 1**.** The fluid is assumed to flow in the $z > 0$ plane with the sheet elongating with a constant flow speed of $U_0 = bx$,where is $b > 0$ is invariant. The velocity components in the cartesian plane are assumed to be u, v, w in the $x, y \,\&\, z - direction$.The angular velocity of the flow is treated as Ψ.Further the flow is consistent with both ambient \ wall temperature and concentration.

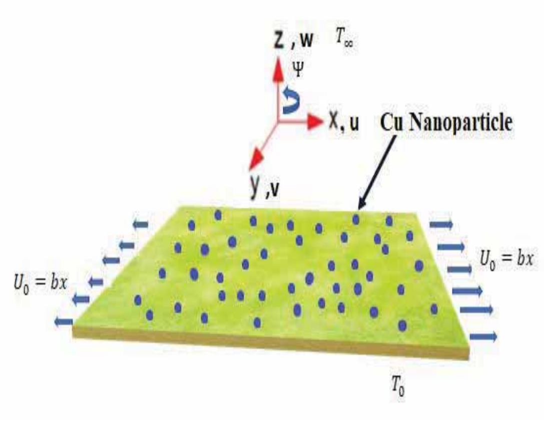

Figure 1. The physical model of the problem

“The **Maxwell-Garnetts and Brinkman models** are used to measure nano liquid thermal conductivity and dynamic viscosity”. These models characterize spherical nanoparticles with a volume fraction of $< 10\%$ .Using the given hypotheses the boundary-layer flow governing equations are[19]

$$\frac{\partial u}{\partial x} + \frac{\partial v}{\partial y} + \frac{\partial w}{\partial z} = 0 \quad (1)$$

$$u\frac{\partial u}{\partial x} + v\frac{\partial u}{\partial y} + w\frac{\partial u}{\partial z} = \frac{\mu_{nf}}{\rho_{nf}}\frac{\partial^2 u}{\partial z^2} + 2\Psi v - \frac{\nu_{nf}}{k_p}u \quad (2)$$

$$u\frac{\partial v}{\partial x} + v\frac{\partial v}{\partial y} + w\frac{\partial v}{\partial z} = \frac{\mu_{nf}}{\rho_{nf}}\frac{\partial^2 v}{\partial z^2} - 2\Psi u - \frac{\nu_{nf}}{k_p}v \quad (3)$$

$$u\frac{\partial T}{\partial x} + v\frac{\partial T}{\partial y} + w\frac{\partial T}{\partial z} = \frac{k_{nf}}{(\rho Cp)_{nf}}\frac{\partial^2 T}{\partial z^2} + \frac{\mu_{nf}}{(\rho Cp)_{nf}}\left[\left(\frac{\partial u}{\partial z}\right)^2 + \left(\frac{\partial v}{\partial z}\right)^2\right] \quad (4)$$

$$u\frac{\partial C}{\partial x} + v\frac{\partial C}{\partial y} + w\frac{\partial C}{\partial z} = D_{nf}\frac{\partial^2 C}{\partial z^2} \quad (5)$$

The end constraints are,

$$u = U_0 \;\; ; v = 0 \;\; ; w = 0 \;\; ; T = T_0 \;\; ; C = C_0 \;\; at \;\; z = 0$$
$$u \to 0; v \to 0; w \to 0; \;\; T \to T_\infty \;\; ; C \to C_\infty \;\; as \;\; z \to \infty \quad (6)$$

μ_{nf} the dynamic viscosity[20] , $\rho_{nf}$the density[21] , k_{nf} the thermal conductivity[22], $(\rho Cp)_{nf}$ the heat capacitance[23], D_{nf} is the mass diffusivity[24] of the NF which are given by

$$\mu_{nf} = \frac{\mu_f}{(1-\phi)^{\frac{5}{2}}}, \qquad \rho_{nf} = (1-\phi)\rho_f + \phi\rho_s \quad (7)$$

$$k_{nf} = k_f\left[\frac{k_s + 2k_f - 2\phi(k_f - k_s)}{k_s + 2k_f + \phi(k_f - k_s)}\right] \quad (8)$$

$$(\rho C_p)_{nf} = (1-\phi)(\rho C_p)_f + \phi(\rho C_p)_s \quad (9)$$

$$D_{nf} = \frac{D_f}{1-\phi}, \quad (10)$$

The subscripts in the above equations indicate the properties of the NF, base fluid(water), solid Cu nanoparticle. The thermophysical properties required for the flow analysis are given below,

TABLE I.
Properties of Water and Solid Copper Nano PARTICLE [25]

Properties	Base Fluid **(Water)**	Nano Particles **(Cu)**
$\boldsymbol{Thermal\ Conductivity(k)(Wm^{-1}K^{-}}$	0.613	400
$\boldsymbol{Density(\rho)(kgm^{-3})}$	997.1	8933
Specific heat $\boldsymbol{(Cp)(Jkg^{-1}K^{-1})}$	4179	385
$\boldsymbol{\beta\ (1/K)}$	36.2x 10^{-5}	1.67x10^{-5}

III. Mathematical Technique

Let us consider the following similarity transformations [19], [22], [26]

$$\left.\begin{array}{l} \eta = \sqrt{\frac{a}{\nu}}z, u = axF'(\eta), v = axG(\eta), \\ w = -\sqrt{a\nu}F(\eta), \Theta(\eta) = \frac{T-T_\infty}{T_0-T_\infty}, \\ \Phi(\eta) = \frac{C-C_\infty}{C_0-C_\infty} \end{array}\right\} \quad (11)$$

Substituting these into the equations to**,** equation **(*1*)** is satisfied and the remaining equations **(*2*)-(*5*)**, along with the boundary conditions**(*6*)**, transform into highly non-linear ODE, which can be given as

$$\frac{\mu_{nf}}{\mu_f}\frac{\rho_f}{\rho_{nf}}F''' = (F')^2 - FF'' - 2R_0G + k_1F' \quad (12)$$

$$\frac{\mu_{nf}}{\mu_f}\frac{\rho_f}{\rho_{nf}}G'' = F'G - G'F + 2R_0F' + k_1G \quad (13)$$

$$\frac{k_{nf}}{k_f}\frac{(\rho C_p)_f}{(\rho C_p)_{nf}}[\Theta''] = -(Pr\,(F\Theta' + Ec((F'')^2 + (G')^2)) \quad (14)$$

$$\Phi'' + \frac{Sc}{(1-\phi)}F\Phi' = 0 \quad (15)$$

With the BCs,

$$\begin{array}{c} F'(\eta) = 1, G(\eta) = 0, F(\eta) = 0, \\ \Theta(\eta) = 1, \Phi(\eta) = 1 \ at\ \eta = 0 \\ F'(\eta) \longrightarrow 0, G(\eta) \longrightarrow 0, \\ \Theta(\eta) \longrightarrow 0, \Phi(\eta) \longrightarrow 0 \ as\ \eta \longrightarrow \infty \end{array} \quad (16)$$

The parameters involved in the above equations are [19],[27]

$$Eckert\ number: \ Ec = \frac{\rho_f U_0^2}{(\rho C_p)_f(T_\infty - T_0)},$$

$$Porosity\ parameter: k_1 = \frac{\nu_f}{bk_p}$$

$$Rotational\ parameter: R_0 = \frac{\Psi}{b}$$

$$Prandtl\ number: Pr = \frac{\upsilon_f}{\alpha_f},$$

$$Schmidt\ number: Sc = \frac{\upsilon_f}{D_f}$$

The expression for the local drag force coefficients [19] C_{fx} *and* C_{fy}, heat transfer coefficient Nu_x and the mass transfer coefficient Sh_x can be defined as

$$C_{fx} \equiv \frac{\tau_{xz}}{\frac{1}{2}\rho U_0^2}, C_{fy} \equiv \frac{\tau_{yz}}{\frac{1}{2}\rho U_0^2},$$

$$Nu = \frac{xq_w}{k(T_0 - T_\infty)}, and$$

$$Sh_x = \frac{xq_m}{D_M(C_0 - C_\infty)}$$

In which τ_{xz}, τ_{yz} signify the tensors of shear stress and q_w , q_m represent "the heat and mass flux at the sheet walls". Applying the transformations**,** the above expressions transform into,

$$\begin{array}{c} Re_x^{\frac{1}{2}}C_{fx} = \frac{\mu_{nf}}{\mu_f}F''(0) \\ Re_x^{1/2}C_{fy} = \frac{\mu_{nf}}{\mu_f}G'(0) \\ Re_x^{-1/2}Nu_x = -\frac{k_{nf}}{k_f}\Theta'(0) \\ Re_x^{-1/2}Sh_x = -\frac{D_{nf}}{D_f}\Phi'(0) \end{array} \quad (17)$$

IV. Solution Methodology

The non-dimensional ODEs are set into a linear format using the relations,

$$f_1 = F, f_2 = F', f_3 = F'', F''' = f_3' = -A_1A_2[f_1f_3 + 2R_0g_1 - (f_2)^2 + k_1f_2] \quad (18)$$

$$g_1 = G, g_2 = G', G'' = g_2' = A_1A_2[-f_1g_2 + 2R_0f_1 + f_2g_1 + k_1g_1] \quad (19)$$

$$\theta_1 = \Theta(\eta), \theta_2 = \Theta'(\eta), \theta_3 = \Theta'_2 = -\frac{Pr * k_f}{k_{nf}}[A_3f_1\theta_2 + Ec[f_3^2 + g_2^2]] \quad (20)$$

$$\Phi_1 = \Phi, \Phi_2 = \Phi', \Phi_3 = -\frac{Scf\Phi'}{(1-\phi)} \quad (21)$$

$$Here, A_1 = \frac{\mu_f}{\mu_{nf}}, \boldsymbol{A_2} = \frac{\rho_{nf}}{\rho_f}, \boldsymbol{A_3} = \frac{[\rho c_p]_{nf}}{[\rho c_p]_f} \quad (22)$$

Along with the modified BCs

$$f_1 = 0, f_2 = 1, g_1 = 0, \Theta_1 = 1, \Phi_1 = 1\ as\ \eta = 0$$

$$f_2 \rightarrow 0, g_1 \longrightarrow 0, \Theta_1 \longrightarrow 0, \Phi_1 \longrightarrow 0\ as\ \eta \longrightarrow 0$$

The set of equations **(*12*)-(*15*)**, along with the prescribed conditions **(16)**, has been solved using the bvp4c solver which performs the finite difference code that implements the three-stage Lobatto IIIA formula of fourth-order [28]. The system is solved with absolute and relative accuracy of order 10^{-6}.

The MATLAB BVP4C implements Lobatto IIIa collocation RK method [29]– [33] . The validation of the code was verified by comparing the results by determining the values of C_{fx}, C_{fy} *and* Nu_x for the base fluid and matched with the formerly available papers in **TABLE 4** and TABLE 3

E-ISSN 2581 – 7957
P-ISSN 2277 – 3916

DOI: 10.32377/cvrjst2418

TABLE II.
COMPARISON OF THE VALUES OF $Re_x^{1/2}C_{fx}$ and $Re_x^{1/2}C_{fy}$ FOR BASE FLUID WHEN $\phi = Ri = A = B = Sc = 0$

	Nor Azizah Yacob et al[34]		N. A. Salleh,.et al[35]		Present findings	
R_0	$-\frac{\mu_{nf}}{\mu_f}F''(0)$	$-\frac{\mu_{nf}}{\mu_f}G'(0)$	$-\frac{\mu_{nf}}{\mu_f}F''(0)$	$-\frac{\mu_{nf}}{\mu_f}G'(0)$	$-\frac{\mu_{nf}}{\mu_f}F''(0)$	$-\frac{\mu_{nf}}{\mu_f}G'(0)$
0.0	1.00000	0.00000	1.000000	0.000000	1.00000	0.000000
0.5	1.13838	0.51276	1.138381	0.512760	1.138411	0.512802
1.0	1.32503	0.83809	1.325029	0.837098	1.325031	0.837121
2.0	1.6524	1.28726	1.652352	1.287259	1.652392	1.287301

TABLE III.
COMPARISON OF CALCULATED VALUES OF $Re_x^{-0.5}Nu_x$ FOR BASE FLUID.

	Nadeem et al. [36]	N. A. Salleh,.et al [35]	Current findings
R_0	$\frac{-k_{nf}}{k_f}\Theta'(0)$	$\frac{-k_{nf}}{k_f}\Theta'(0)$	$\frac{-k_{nf}}{k_f}\Theta'(0)$
0.00	1.770948	1.770948	1.77094791
0.50	1.725631	1.725631	1.72563892
1.00	1.660286	1.660286	1.66028591
2.00	1.533487	1.533487	1.53348701

V. RESULTS AND DISCUSSION

To analyse the predominance of the parameters such as Eckert number, porosity etc involved in the governing ODEs of the rotary NF flow over a linearly stretching sheet in the presence of internal energy and porous medium the Lobatto IIIA collocation method has been utilised . The results obtained have been graphed, tabulated, and discussed below.

The values of parameters throughout the analysis have been considered as $Ec = 0.2, k_1 = 0.5, Sc = 0.5, R_0 = 0.2, \phi = 0.02$, except for the modifications required in the corresponding figures.

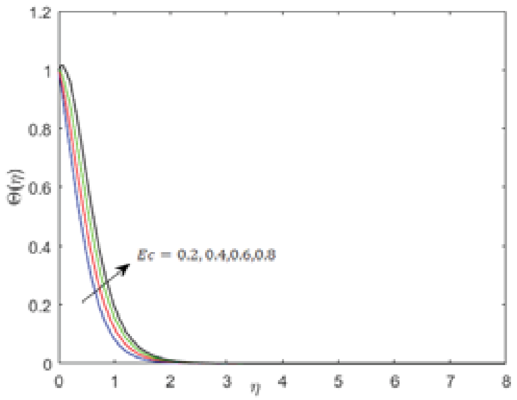

Figure 2. Effect of Eckert number on the Temperature profile

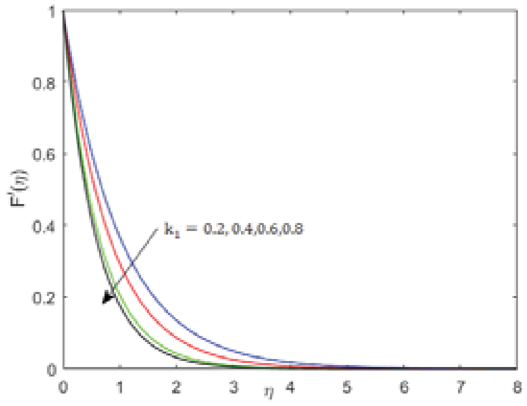

Figure 3. The Predominance of k_1 (porosity parameter) value on PVG

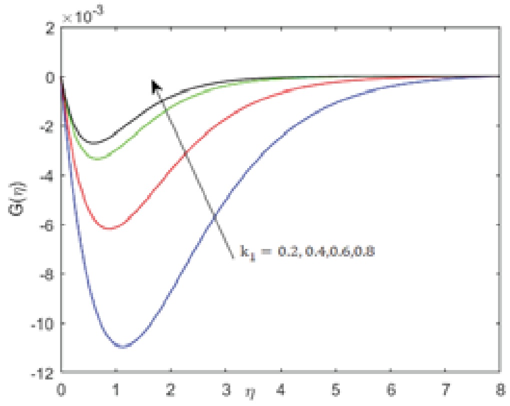

Figure 4. Impact of k_1 on the SVG

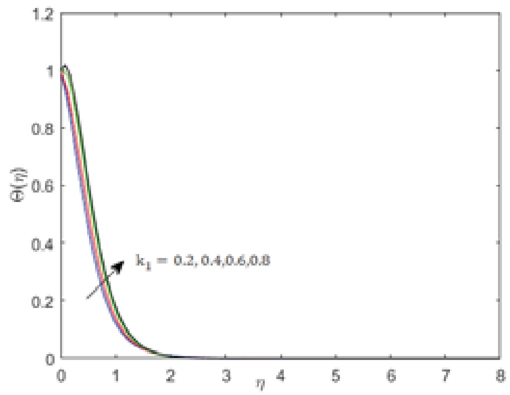

Figure 5. Effect of k_1 on $\Theta(\eta)$

E-ISSN 2581 – 7957
P-ISSN 2277 – 3916

DOI: 10.32377/cvrjst2418

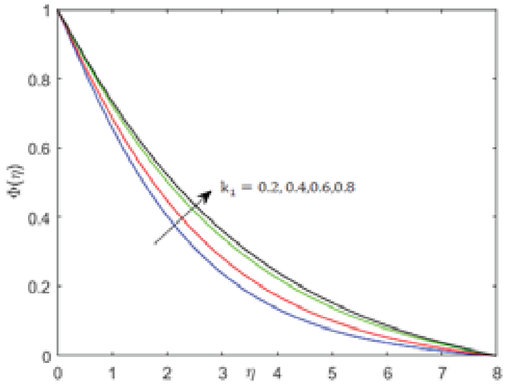

Figure 6. Effect of k_1 on $\Phi(\eta)$

Figure 3-Figure 6 demonstrates the porosity parameter's role on the physical properties of the NF flow. Higher porosity increases the impulse and speeds the flow, whereas it decelerates the flow for small pore size by increasing the "viscous drag of the porous channel" [37]. Thus, the improvement in values of k_1 leads to the enlargement of the temperature, SVG, and concentration profiles whereas the impact is opposite on PVG. And also, we observe that the increase in the porosity leads to the increase in both temperature and concentration profiles.

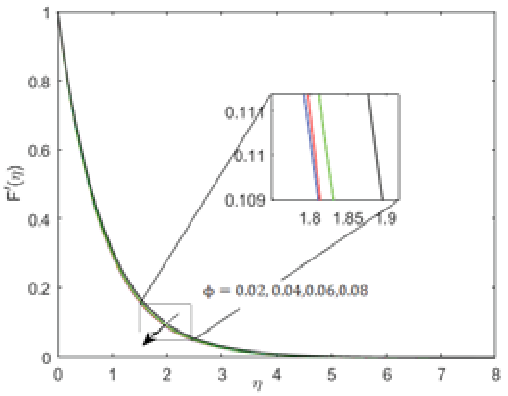

Figure 7. Influence of ϕ on primary velocity $F'(\eta)$

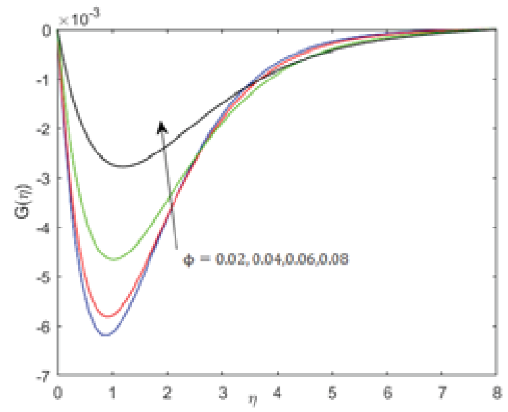

Figure 8. Development of secondary velocity profile with improvement in ϕ

The predominance of the solid Cu – "nanoparticle volume fraction" on flow properties of fluid flow is displayed in Figure 7-Figure 10**.** From the graphs, it is evident that the addition of the nanoparticle into the base fluid enhances the temperature and decreases the mass diffusivity of the flow. We notice the improvement in the secondary velocity profiles and fall in PVG due to the increase in ϕ.

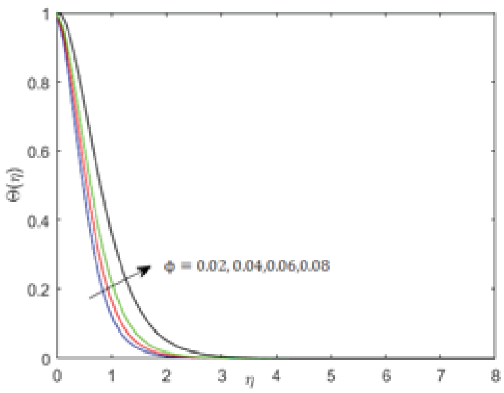

Figure 9. The upshoot of temperature with change in ϕ

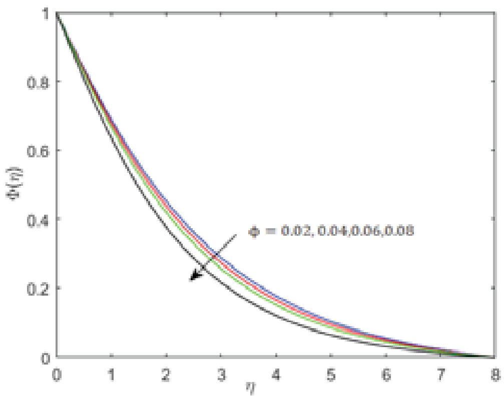

Figure 10. The variation in the concentration profile with ϕ

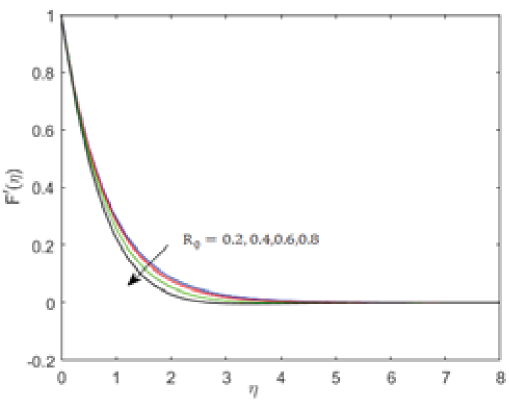

Figure 11. Impact of R_0 on $F'(\eta)$

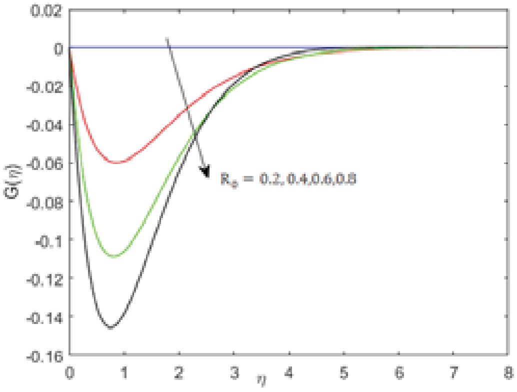

Figure 12. The change in $G(\eta)$ with changes in R_0

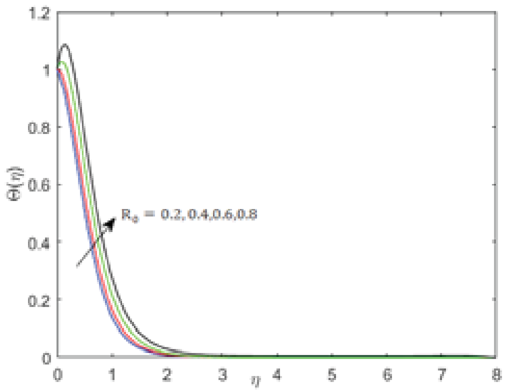

Figure 13. Impact of R_0 on $\Theta(\eta)$

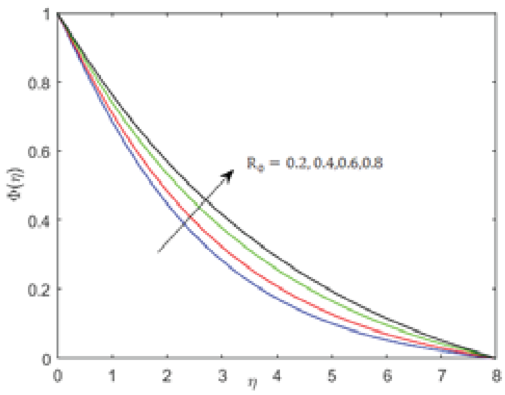

Figure 14. The influence of R_0 on $\Phi(\eta)$

Figure 11-Figure 14 shows the influences of the rotation parameter on the velocity, concentration, and temperature BLs of the NF fluid flow. The statistics display that the increase in the R_0 value improvises the concentration and the temperature of the flow but leads to the downfall of the speed of the fluid. Increasing the rotation generally causes the particle motion close to the boundary to slow down. These factors contribute to the rise in temperature and concentration profiles.

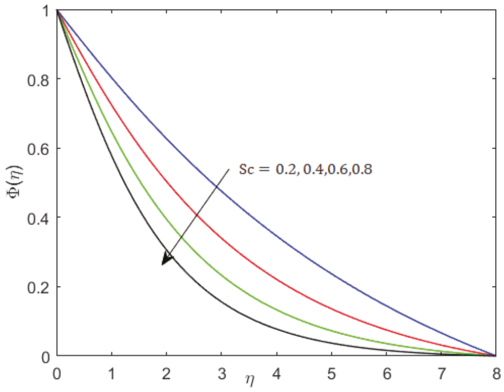

Figure 15. The outcome of Sc's effect on $\Phi(\eta)$

Schmidt number is the ratio of the shear component for diffusivity viscosity/density to the mass-transfer diffusivity. This equation materially connects the hydrodynamic and the mass-transfer BLs. Thus, from Figure 15 we understand that the rise in Sc diminishes the concentration profile.

TABLE 4. displays the numerical values of the physical quantities of industrial interest for various values of the parameters involved in the modified flow governing equations. From the table, we observe that the improvement in Ec leads to the fall in local Nusselt number due to the reason that the rise Ec results in the fall in thermal BL. The enlargement of the values of k_1 *and* R_0 lead to the fall local Sherwood number values, whereas we observe the opposite behaviour when the ϕ *and* Sc values increase as seen from the tabulated value. The primary and secondary skin friction values improve with k_1 and decay for the rise in the values of ϕ *and* R_0

E-ISSN 2581 – 7957
P-ISSN 2277 – 3916
CVR Journal of Science and Technology, Volume 24, June 2023
DOI: 10.32377/cvrjst2418

TABLE IV.
CALCULATED VALUES OF $\frac{1}{(1-\phi)^{2.5}}F''(0)$, $\frac{1}{(1-\phi)^{2.5}}G'(0)$, $-\frac{k_{nf}}{k_f}\Theta'(0)$ AND $-\frac{1}{(1-\phi)}\Phi'(0)$ FOR DIFFERENT VALUES OF THE PHYSICAL PARAMETERS SUCH AS Ec, Sc, R_0, ϕ *and* k_1

R_0	Ec	Sc	ϕ	k_1'	$Re_x^{1/2}C_{fx}$	$Re_x^{1/2}C_{fy}$	$Re_x^{-1/2}Nu_x$	$Re_x^{-1/2}Sh_x$
0	0.5	0.5	0.5	0.5	-1.111816	0	0.41709	0.345995
0.2					-1.288031	-0.171253	0.364229	0.334726
0.4					-1.303946	-0.193361	0.290194	0.329548
0.6					-1.34511	-0.370777	0.098932	0.317088
0.8					-1.400148	-0.52773	-0.156678	0.302363
0.2	**0.2**	0.2	0.02	0.5	-1.288196	-0.019665	1.296906	0.327212
	0.4				-1.288196	-0.019665	0.674597	0.327212
	0.6				-1.288196	-0.019665	0.052309	0.327212
	0.8				-1.288196	-0.019665	-0.570017	0.327212
0.2	0.5	0.5	**0.02**	0.5	-1.224904	-0.018701	0.402254	0.330155
			0.04		-1.288197	-0.019665	0.36346	0.334671
			0.06		-1.354621	-0.020648	0.32121	0.339555
			0.08		-1.424474	-0.021652	0.275239	0.344818
0.2	0.5	0.5	0.02	**0**	-1.052069	-0.026512	0.78951	0.366961
				0.5	-1.288197	-0.019665	0.36346	0.334671
				1	-1.662988	-0.014328	-0.343836	0.295102
				1.5	-1.821711	-0.012902	-0.651519	0.281863
0.2	0.5	**0.2**	0.02	0.5	-1.288197	-0.019665	0.36346	0.201807
		0.4			-1.288197	-0.019665	0.36346	0.289629
		0.6			-1.288197	-0.019665	0.36346	0.379276
		0.8			-1.288197	-0.019665	0.36346	0.465216

VI. Conclusions

The 3D rotational flow of $Cu + water$ NF across an elongating sheet is studied to examine the effects of viscous dissipation and porosity on fluid flow parameters. We utilised the Lobatto IIIa fourth-order approach in MATLAB to evaluate the data. We next analysed the data mathematically and visually. The following are the paper's main takeaways:

- The SVG amplifies with the boost in ϕ , and k_1 whereas the PVG displays the opposite effect.
- With the amplification of the rotation parameter, nanoparticle volume fraction, internal energy and k_1 the temperature of the fluid experiences an improvement
- The local Nusselt number declines with an increase in the Eckert number.
- The surge in the Schmidt number improves the rate of diffusivity and decreases the concentration of the species.

References

[1] M. Gnaneswara Reddy, P. Padma, and B. Shankar, "Effects of viscous dissipation and heat source on unsteady MHD flow over a stretching sheet," *Ain Shams Eng. J.*, vol. 6, no. 4, pp. 1195–1201, Dec. 2015, doi: 10.1016/j.asej.2015.04.006.

[2] B. Gebhart, "Effects of viscous dissipation in natural convection," *J. Fluid Mech.*, vol. 14, no. 2, pp. 225–232, Oct. 1962, doi: 10.1017/S0022112062001196.

[3] A. Hussanan, M. Z. Salleh, I. Khan, and S. Shafie, "Analytical solution for suction and injection flow of a viscoplastic Casson fluid past a stretching surface in the presence of viscous dissipation," *Neural Comput. Appl.*, vol. 29, no. 12, pp. 1507–1515, 2018, doi: 10.1007/s00521-016-2674-0.

[4] N. S. Yusof, S. K. Soid, M. R. Illias, A. S. Abd Aziz, and N. A. A. Mohd Nasir, "Radiative Boundary Layer Flow of Casson Fluid Over an Exponentially Permeable Slippery Riga Plate with Viscous Dissipation," *J. Adv. Res. Appl. Sci. Eng. Technol.*, vol. 21, no. 1, pp. 41–51, 2020, doi: 10.37934/araset.21.1.4151.

[5] M. Shoaib *et al.*, "Numerical analysis of 3-D MHD hybrid nanofluid over a rotational disk in presence of thermal radiation with Joule heating and viscous dissipation effects using Lobatto IIIA technique," *Alexandria Eng. J.*, vol. 60, no. 4, pp. 3605–3619, 2021, doi: 10.1016/j.aej.2021.02.015.

[6] T. Salahuddin, N. Siddique, M. Arshad, and I. Tlili, "Internal energy change and activation energy effects on Casson fluid," *AIP Adv.*, vol. 10, no. 2, 2020, doi: 10.1063/1.5140349.

[7] T. M. Ajayi, A. J. Omowaye, and I. L. Animasaun, "Viscous Dissipation Effects on the Motion of Casson Fluid over an Upper Horizontal Thermally Stratified Melting Surface of a Paraboloid of Revolution: Boundary Layer Analysis," *J. Appl. Math.*, 2017, doi: 10.1155/2017/1697135.

[8] I. A. Badruddin, Z. A. Zainal, Z. A. Khan, and Z. Mallick, "Effect of viscous dissipation and radiation on natural convection in a porous medium embedded within vertical annulus," *Int. J. Therm. Sci.*, vol. 46, no. 3, pp. 221–227, 2007, doi: 10.1016/j.ijthermalsci.2006.05.005.

[9] X. Q. Wang and A. S. Mujumdar, "Heat transfer characteristics of nanofluids: a review," *Int. J. Therm. Sci.*, vol. 46, no. 1, pp. 1–19, 2007, doi: 10.1016/j.ijthermalsci.2006.06.010.

[10] M. Tayyab, I. Siddique, F. Jarad, M. K. Ashraf, and B. Ali, "Numerical solution of 3D rotating nanofluid flow subject to Darcy-Forchheimer law, bio-convection and activation energy," *South African J. Chem. Eng.*, vol. 40, no. January, pp. 48–56, 2022, doi: 10.1016/j.sajce.2022.01.005.

[11] K. Zaimi, A. Ishak, and I. Pop, "Stretching surface in rotating viscoelastic fluid," *Appl. Math. Mech.*, vol. 34, no. 8, pp. 945–952, Aug. 2013, doi: 10.1007/s10483-013-1719-9.

[12] S. A. Bakar, N. M. Arifin, R. Nazar, F. M. Ali, and I. Pop, "Forced convection boundary layer stagnation-point flow in Darcy-Forchheimer porous medium past a shrinking sheet," *Front. Heat Mass Transf.*, vol. 7, no. 1, pp. 1–6, 2016, doi: 10.5098/hmt.7.38.

[13] I. Ullah, S. Shafie, and I. Khan, "Effects of slip condition and Newtonian heating on MHD flow of Casson fluid over a nonlinearly stretching sheet saturated in a porous medium, Effects of slip condition and Newtonian heating," *J. King Saud Univ. - Sci.*, vol. 29, no. 2, pp. 250–259, 2017, doi: 10.1016/j.jksus.2016.05.003.

[14] A. Tassaddiq, "Impact of Cattaneo-Christov heat flux model on MHD hybrid nano-micropolar fluid flow and heat transfer with viscous and joule dissipation effects," *Sci. Rep.*, vol. 11, no. 1, pp. 1–14, 2021, doi: 10.1038/s41598-020-77419-x.

[15] K. A. Maleque, "Dufour and soret effects on unsteady MHD convective heat and mass transfer flow due to a rotating disk," *Lat. Am. Appl. Res.*, vol. 40, no. 2, pp. 105–111, 2010.

[16] S. Dero, A. M. Rohni, and A. Saaban, "Triple Solutions and Stability Analysis of Mixed Convection Boundary Flow of Casson Nanofluid over an Exponentially Vertical Stretching / Shrinking Sheet," vol. 1, no. 1, pp. 94–110, 2020.

[17] T. S. Kumar, "Hybrid nanofluid slip flow and heat transfer over a stretching surface," *Partial Differ. Equations Appl. Math.*, vol. 4, p. 100070, Dec. 2021, doi: 10.1016/j.padiff.2021.100070.

[18] A. O. Ajibade, A. M. Umar, and T. M. Kabir, "An analytical study on effects of viscous dissipation and suction/injection on a steady mhd natural convection couette flow of heat generating/absorbing fluid," *Adv. Mech. Eng.*, vol. 13, no. 5, pp. 1–12, 2021, doi: 10.1177/16878140211015862.

[19] W. Owhaib, M. Basavarajappa, and W. Al-Kouz, "Radiation effects on 3D rotating flow of Cu-water nanoliquid with viscous heating and prescribed heat flux using modified Buongiorno model," *Sci. Rep.*, vol. 11, no. 1, p. 20669, 2021, doi: 10.1038/s41598-021-00107-x.

[20] H. F. Oztop and E. Abu-Nada, "Numerical study of natural convection in partially heated rectangular enclosures filled with nanofluids," *Int. J. Heat Fluid Flow*, vol. 29, no. 5, pp. 1326–1336, 2008, doi: 10.1016/j.ijheatfluidflow.2008.04.009.

[21] S. Chaudhary and K. M. Kanika, "Viscous dissipation and Joule heating in MHD Marangoni boundary layer flow and radiation heat transfer of Cu–water nanofluid along particle shapes over an exponential temperature," *Int. J. Comput. Math.*, vol. 97, no. 5, pp. 943–958, 2020, doi: 10.1080/00207160.2019.1601713.

[22] B. C. Rout, S. R. Mishra, and T. Thumma, "Effect of viscous dissipation on Cu-water and Cu-kerosene nanofluids of axisymmetric radiative squeezing flow," *Heat Transf. - Asian Res.*, vol. 48, no. 7, pp. 3039–3054, 2019, doi: 10.1002/htj.21529.

[23] U. Khan, N. Ahmed, M. Asadullah, and S. Tauseef Mohyud-din, "Effects of viscous dissipation and slip velocity on two-dimensional and axisymmetric squeezing flow of Cu-water and Cu-kerosene nanofluids," *Propuls. Power Res.*, vol. 4, no. 1, pp. 40–49, 2015, doi: 10.1016/j.jppr.2015.02.004.

[24] U. Khan, A. Zaib, I. Khan, and K. S. Nisar, "Activation energy on MHD flow of titanium alloy (Ti6Al4V) nanoparticle along with a cross flow and streamwise direction with binary chemical reaction and non-linear radiation: Dual Solutions," *J. Mater. Res. Technol.*, vol. 9, no. 1, pp. 188–199,

2020, doi: 10.1016/j.jmrt.2019.10.044.

[25] W. Owhaib, M. Basavarajappa, and W. Al-Kouz, "Radiation effects on 3D rotating flow of Cu-water nanoliquid with viscous heating and prescribed heat flux using modified Buongiorno model," *Sci. Rep.*, vol. 11, no. 1, pp. 1–16, 2021, doi: 10.1038/s41598-021-00107-x.

[26] T. Hayat, M. Imtiaz, and A. Alsaedi, "Melting heat transfer in the MHD flow of Cu–water nanofluid with viscous dissipation and Joule heating," *Adv. Powder Technol.*, vol. 27, no. 4, pp. 1301–1308, 2016, doi: 10.1016/j.apt.2016.04.024.

[27] H. M. Duwairi and R. A. Damseh, "Magnetohydrodynamic natural convection heat transfer from radiate vertical porous surfaces," *Heat Mass Transf. und Stoffuebertragung*, vol. 40, no. 10, pp. 787–792, 2004, doi: 10.1007/s00231-003-0476-2.

[28] A. S. Oke, "Heat and Mass Transfer in 3D MHD Flow of EG-Based Ternary Hybrid Nanofluid Over a Rotating Surface," *Arab. J. Sci. Eng.*, 2022, doi: 10.1007/s13369-022-06838-x.

[29] L. O. Jay, "Lobatto Methods," *Encycl. Appl. Comput. Math.*, vol. 1, no. 1, pp. 817–826, 2015, doi: 10.1007/978-3-540-70529-1_123.

[30] S. G. Pinto, S. P. Rodríguez, and J. I. M. Torcal, "On the numerical solution of stiff IVPs by Lobatto IIIA Runge-Kutta methods," *J. Comput. Appl. Math.*, vol. 82, no. 1–2, pp. 129–148, 1997, doi: 10.1016/s0377-0427(97)00086-1.

[31] C. Ouyang, R. Akhtar, M. A. Z. Raja, M. Touseef Sabir, M. Awais, and M. Shoaib, "Numerical treatment with Lobatto IIIA technique for radiative flow of MHD hybrid nanofluid (Al2O3-Cu/H2O) over a convectively heated stretchable rotating disk with velocity slip effects," *AIP Adv.*, vol. 10, no. 5, 2020, doi: 10.1063/1.5143937.

[32] A. S. Alhamaly, M. Khan, S. Z. Shuja, B. S. Yilbas, and H. Al-Qahtani, "Axisymmetric stagnation point flow on linearly stretching surfaces and heat transfer: Nanofluid with variable physical properties," *Case Stud. Therm. Eng.*, vol. 24, Apr. 2021.

[33] N. Vedavathi, G. Dharmaiah, K. Venkatadri, and S. A. Gaffar, "Numerical study of radiative non-Darcy nanofluid flow over a stretching sheet with a convective Nield conditions and energy activation," *Nonlinear Eng.*, vol. 10, no. 1, pp. 159–176, 2021, doi: 10.1515/nleng-2021-0012.

[34] N. A. Yacob, N. F. Dzulkifli, S. N. A. Salleh, A. Ishak, and I. Pop, "Rotating flow in a nanofluid with cnt nanoparticles over a stretching/shrinking surface," *Mathematics*, vol. 10, no. 1, 2022, doi: 10.3390/math10010007.

[35] S. N. A. Salleh, N. Bachok, and N. M. Arifin, "Flow and Heat Transfer Towards a Stretching Surface in a Rotating Nanofluid with Suction," *Indian J. Sci. Technol.*, vol. 9, no. 48, 2017, doi: 10.17485/ijst/2016/v9i48/97772.

[36] S. Nadeem, A. U. Rehman, and R. Mehmood, "Boundary Layer Flow of Rotating Two Phase Nanofluid Over a Stretching Surface," *Heat Transf. - Asian Res.*, vol. 45, no. 3, pp. 285–298, 2016, doi: 10.1002/htj.21167.

[37] C. Kang and P. Mirbod, "Porosity effects in laminar fluid flow near permeable surfaces," *Phys. Rev. E*, vol. 100, no. 1, p. 013109, Jul. 2019, doi: 10.1103/PhysRevE.100.013109.